

Sensitivity of photodissociation rate coefficients and O₃ photochemical tendencies to aerosols and clouds

Huiyan Yang

Atmospheric and Oceanic Sciences Program, Princeton University, Princeton, New Jersey, USA

Hiram Levy II

Geophysical Fluid Dynamics Laboratory, Princeton, New Jersey, USA

Received 18 May 2004; revised 11 August 2004; accepted 26 August 2004; published 17 December 2004.

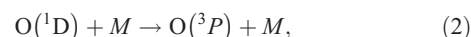
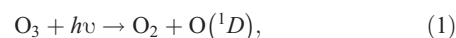
[1] We examine the sensitivity of the daily integrated photodissociation rate (DIPR) coefficients of O₃(O¹D) and NO₂, the daily averaged O₃ photochemical tendency, and OH concentration to variations of clouds and of four aerosol components: black carbon (BC), mineral dust, sea salt, and sulfate. Clouds and BC aerosols are found to be the most important. A comparison between the sensitivity study and some representative observations showed that the global average cloud reduction of DIPR at the surface level is ~20% and it is ~30% in storm track zones. At the surface level the average negative BC impact is ~10% in urban areas and could reach ~40% in some heavily polluted urban areas. Mineral dust aerosol, which is the next most important, can reduce the photochemistry at the surface level by over 17% in some seasons over the desert or along its long-range transport paths. The negative impact of sulfate aerosols is around 2% at the surface level, and the impact is as positive as 4% at the top of the sulfate aerosol layer in some urban areas. BC, sulfate, and mineral dust all have much smaller impacts away from their source regions. The impact of sea-salt aerosol is generally less than 1%. While the fractional impacts on O₃ production and destruction and OH concentration do not depend much on NO_x, the magnitude of the impact on O₃ chemical tendency and OH concentration depends strongly on the concentration of NO_x: When NO_x is very low, the impacts are also very small even if DIPRs are strongly affected. Different mixing states of absorbing and scattering aerosol components, external, coating, and internal, are studied. It is found that with the same amount of each component, the external mixing state produces the weakest impact while the internal mixing state produces the strongest impact. Coating has almost the same impact as internal mixing. There is very little synergy between cloud and absorbing aerosols when clouds are located above the aerosol. The aerosol absorption is strengthened when clouds and aerosol are located in the same layer. The synergy is strong when clouds are located below the absorbing aerosol, where the impact of absorbing aerosol dominates. *INDEX TERMS*: 0305 Atmospheric Composition and Structure: Aerosols and particles (0345, 4801); 0317 Atmospheric Composition and Structure: Chemical kinetic and photochemical properties; 0320 Atmospheric Composition and Structure: Cloud physics and chemistry; *KEYWORDS*: photochemical impacts of aerosol, tropospheric photochemistry, aerosol optical properties, black carbon aerosol, aerosol mixing states, synergy between aerosol and cloud

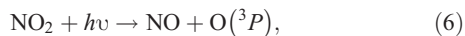
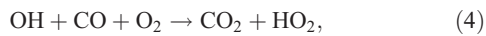
Citation: Yang, H., and H. Levy II (2004), Sensitivity of photodissociation rate coefficients and O₃ photochemical tendencies to aerosols and clouds, *J. Geophys. Res.*, 109, D24301, doi:10.1029/2004JD005032.

1. Introduction

[2] We study the aerosol and cloud photochemical impacts on tropospheric chemistry, because they can absorb and/or scatter solar radiation, which alters solar photon distribution and thus affects the photodissociation rate coefficients J . The heterogeneous reactions on aerosol and cloud particles [Seinfeld and Pandis, 1998] are not addressed in this paper.

[3] When J is changed, the whole chemistry system will be changed. For example, in the simple CO-NO_x-O₃ system, the main reactions are





[4] By assuming that $O(^1D)$ and $O(^3P)$ are in steady states, one gets an O_3 net tendency proportional to the J of NO_2 . A similar analysis shows that the concentration of OH is proportional to the J of O_3 by assuming that OH is also in the steady state.

[5] Cloud impacts on J [e.g., *Madronich, 1987; Krol and Weele, 1997; Matthijsen et al., 1998*] have been studied by many researchers. Similar cloud optical parameterizations have been applied in these studies, and thus similar conclusions were achieved. In contrast, aerosols have been parameterized differently by different researchers. For example, *He and Carmichael [1999]* studied the sensitivity of the NO_2 photodissociation rate coefficient and O_3 production to four types of aerosols. They specified a fixed mixing ratio among different components for each type, and applied an external mixing assumption. *Liao et al. [1999]* studied the impacts of sulfate, soot, and mineral dust aerosols on tropospheric photodissociation rates in both clear and cloudy atmospheres. They looked at internal and external mixtures of sulfate and soot. *Martin et al. [2003]* studied the photochemical effects of aerosols from both the radiative and heterogeneous reaction viewpoints, but considered only the external mixing of aerosols.

[6] It was suggested that the BC mixing ratio and mixing state are aerosol size dependent [*Hitzenberger and Puxbaum, 1993; Berner et al., 1996*]: BC is much more enriched in the finer particle range than the larger particle range, and it is externally mixed in the finer particle range and internally mixed in the larger particle range. Because the mixing ratio and mixing state of absorbing and scattering aerosol components determine the optical properties of the aerosol [*Ackerman and Toon, 1981; Bergstrom et al., 1982; Chylek et al., 1984; Jacobson, 2001*], and because we prescribe a static size distribution for each aerosol component as other researchers [e.g., *He and Carmichael, 1999; Liao et al., 1999*], we did numerical experiments for each of the four main aerosol components separately. We then did experiments to assess the importance of different mixing states of BC on J values: external mixing, internal mixing, and coating as a special case of internal mixing. To better understand the results of the sensitivity study, we convert the aerosol optical depth to mass loading, and compare it with measurements to see the range of aerosol impacts. We also examined the variation of chemical terms under different NO_x concentration, which reveals a wide range for the same aerosol or cloud loading. Cloud impacts are studied in this paper to compare their impacts with aerosols, and to assess the synergy between clouds and absorbing aerosols.

[7] We look at the sensitivity of the daily integrated photodissociation rate (DIPR) as did *Krol and Weele [1997]* instead of J at different solar zenith angle for two reasons. First, although the fractional change of J is larger, the absolute value of J is much smaller [e.g., *Liao et al.,*

1999] at large solar zenith angle. Second, our interest is in the climatic effect of cloud and aerosols on J and chemistry, so a daily average or integrated value is more appropriate than an instantaneous value.

[8] The sensitivities of DIPR of $O_3(^1D)$ and NO_2 were selected because they are critical to tropospheric chemistry. Additionally, they represent two distinct types of J . The first is strongly affected and the second is not by the variation of overhead column O_3 absorption, because the upper active wavelength for J of $O_3(^1D)$ is around 325 nm, while it is around 420 nm for J of NO_2 . J of $O_3(^1D)$, HNO_3 and PAN are the first type while J of NO_2 and NO_3 are the second type. The numerical models used in this study are briefly introduced in section 2. The aerosol and cloud optical parameters are given in the first part of section 3 and then the sensitivity study is presented. The synergy between clouds and absorbing aerosol BC is studied at the end of section 3. After identifying BC absorption as a critical photochemical factor in tropospheric chemistry, section 4 discusses its impact under different mixing state assumptions. Section 5 summarizes the whole study.

2. Model Description

[9] The aerosol optical parameters were calculated with Wiscombe's Mie code (<http://climate.gsfc.nasa.gov/%7Ewiscombe/Home.html>). The inputs for the Mie code are aerosol size indices and refractive indices, which are functions of wavelength. The outputs are extinction and scattering efficiencies, and the asymmetry factor. The forward scatter and backscatter amplitude, and information about polarization are also calculated, but are not used in this study. J were calculated with the NCAR Tropospheric Ultraviolet and Visible (TUV) radiation model [*Madronich and Flocke, 1998*] (<http://acd.ucar.edu/models/UV/TUV/index.html>), version 4.0a. TUV is modified to compute the DIPR. Actinic flux was calculated with the eight-stream DISORT radiative transfer scheme in TUV. The wavelength spectrum is divided into 130 uneven intervals from 185 nm to 735 nm (the Isaksen grid in TUV), and the vertical domain is divided into 50 1 km layers from the ground to 50 km.

[10] Daily averaged O_3 tendencies and OH concentrations were calculated with a background photochemical box model [*Klonecki and Levy, 1997; Klonecki, 1999*], which was coupled to TUV. The chemistry mechanism was constructed for the background troposphere and has 29 species and 75 reactions.

3. Sensitivity of Aerosols and Cloud to Tropospheric Chemistry

3.1. Aerosol and Cloud Particle Characteristics

[11] Four components of aerosols: BC, mineral dust, sulfate and oceanic particles are studied. Here "BC" represents the hydrophobic carbonaceous materials that are a product of direct particle emission into the atmosphere by incomplete combustion processes, which can be fossil fuel combustion or biomass burning [e.g., *Cooke et al., 1999*]. The mineral dust is composed of soil-derived minerals [*d'Almeida et al., 1991*]. Sulfate is a mixture of H_2SO_4 , $(NH_4)_2SO_4$, and NH_4HSO_4 , where all three are weak

Table 1. Aerosol Size Distribution Parameters and Refractive Indexes

Aerosol Component	$r_{g,z}$ μm	σ_g	m_r (300 nm)	m_i (300 nm)
BC	0.0118	2.00	1.740	-0.470
Mineral dust	0.5	2.20	1.530	-2.50E-2 ^a
Sulfate	0.0695	2.03	1.469	-1.00E-8
Oceanic	0.3	2.51	1.390	-5.83E-7

^aRead -2.50E-2 as -2.50×10^{-2} .

absorbers but strong scatters [Nemesure *et al.*, 1995; Boucher and Anderson, 1995]. It is thus justified to use one of them to represent sulfate from the radiative transfer viewpoint. In this paper, the refractive index of sulfate is represented by a 75% solution of H_2SO_4 [World Climate Programme, 1986]. Oceanic aerosol is a 30% solution of sea salt [d'Almeida *et al.*, 1991].

[12] The size distribution of each aerosol component is represented by a lognormal function and the related parameters are listed in Table 1 (as d'Almeida *et al.* [1991]). Here r_g is the median radius of the aerosol size distribution, which is also called the mode radius. σ_g is the standard deviation of $\log r$, m_r and m_i are the real and imaginary components of the refractive index. The absolute value of m_i indicates the absorption strength. From Table 1, it can be seen that BC is the strongest absorber, mineral dust is the second strongest absorber, while sulfate and oceanic particles absorb very weakly.

[13] The single-scattering albedo ω , the asymmetry factor g and the extinction cross section σ_e shown in Table 2 are calculated with Wiscombe's Mie code, by employing the above refractive index and size distribution parameters. The results are comparable with those given by d'Almeida *et al.* [1991]. Hygroscopic growth of aerosols, which increases the impacts of sulfate and oceanic aerosols at high humidity [He and Carmichael, 1999], but not BC and mineral dust since the later two are considered to be hydrophobic [Haywood and Shine, 1995; Liao *et al.*, 1999], is not considered in this paper. There is a wavelength dependence of aerosol optical parameters, while cloud optical parameters are assumed to be independent of wavelength, because the size of cloud particle is much larger than the UV and visible wavelength. The aerosol refractive indices, and thus the optical parameters, are from 200 nm to 750 nm, with a wavelength interval of 50 nm. In TUV, the parameters at wavelengths smaller than 200 nm are set the same as those at 200 nm, and parameters at other wavelengths are interpolated. All the optical parameters listed in Table 2 are normalized to 1 particle/cm³. The lognormal size distribution is used to integrate over each size distribution. Sulfate and oceanic aerosols are assumed to be pure scatters because of their weak absorption as shown in Table 1. Cloud particles are also set as pure scatters since water does not absorb in the wavelength interval relevant to tropospheric chemistry. The asymmetry factor of cloud particles is set at 0.85 [e.g., Liao *et al.*, 1999].

[14] The optical depth τ , which will be used in the sensitivity study, is calculated as

$$\tau = \int_{z_1}^{z_2} \sigma_e N(z) dz,$$

where $N(z)$ is the number concentration of aerosol at level z . It is convenient to use optical depth as the unit of aerosol loading in the sensitivity study, but field observations usually measure the aerosol concentration by mass. To make the sensitivity study clearer in the sense of aerosol mass concentration, Table 3 lists the number concentrations and mass concentrations corresponding to the optical depth of 0.1 appearing in the sensitivity study, by assuming a homogeneous aerosol layer of a depth of 2 km. To convert number concentration to mass concentration, one needs the specific volume v of each aerosol component:

$$v = 1/N \int_0^\infty 4/3 \pi r^3 n(r) dr = 4/3 \pi r_v^3.$$

Here, $n(r)$ is the number distribution. The relation between r_v and r_g is $r_v = r_g \exp[(3/2) \ln^2 \sigma_g]$. The mass concentration is calculated as $M = N * \rho * v$.

[15] In the following sensitivity study, the aerosol layer is assumed to have a constant particle number density from the surface to 2 km, and the cloud layer is assumed to be homogenous from 2 km to 4 km, unless specified otherwise. The calculations are performed for 15 July at latitude of 40.5°N. The land surface albedo is set as 0.17 [Rossow and Schiffer, 1991]. The total O_3 column content is set as 300 DU [Brasseur and Solomon, 1986]. CO is set as 103 ppb, O_3 is 50 ppb, and CH_4 is 1.7 ppm [Seinfeld and Pandis, 1998]. The relative humidity is 74% [Peixoto and Oort, 1991]. All these values are selected to represent the background continental surface layer. In the simulations, it is assumed that a high NO_x concentration represents a polluted case and low NO_x represents the background, while the concentrations of other species are kept unchanged.

3.2. Sensitivity to BC Aerosol

[16] BC causes a decrease in J throughout the atmosphere, especially in and below the aerosol layer. Figure 1 shows that a BC aerosol layer with an optical depth of 0.5 decreases the DIPR of $O_3(O^1D)$ and NO_2 by $\sim 48\%$ at ground level. The DIPRs are decreased $\sim 25\%$ at an optical depth of 0.2, and $\sim 14\%$ at an optical depth of 0.1. The impact of BC aerosols decreases rapidly with height in the aerosol layer, because of the accumulated absorption by BC at the lower levels, and reaches an inflection point at the top of aerosol layer, where the fractional change is no more than half of that at the surface level. The impact decreases much slower above the aerosol layer. However, the variation of the DIPR of NO_2 does not change much with height, but the variation of the DIPR of $O_3(O^1D)$ decreases steadily

Table 2. Aerosol and Cloud Optical Parameters at 300 nm

	Single-Scattering Albedo ω	Asymmetry Factor g	Extinction Cross Section σ_e , $\mu\text{m}^2/\text{particle}$
BC	0.3128	0.4537	1.2118E-3
Mineral dust	0.5741	0.9072	5.9971
Sulfate	1.0	0.7086	1.0982E-1
Oceanic	1.0	0.8052	3.5004
Cloud ^a	1.0	0.85	—

^aCloud extinction cross section depends on the size distribution of cloud particles, which is not distinguished in this paper. The bulk optical depth is used directly.

Table 3. Conversion Between Different Aerosol Loading Units

	Particle Mass Density ρ_p^a g/cm ³	Optical Depth τ (300 nm)	Number Concentration, number/cm ³	Mass Concentration M , $\mu\text{g}/\text{m}^3$	Column Burden, g/m ²
BC	2.3	0.1	4.1261E+04	5.6750E+00	1.1350E-02
Mineral dust	2.5	0.1	8.3374E+00	1.7902E+02	3.5805E-01
Sulfate	1.7	0.1	4.5529E+02	1.0387E+01	2.0774E-02
Oceanic	1.375 ^b	0.1	1.4284E+01	1.0107E+02	2.0214E-01

^aFrom *d'Almeida et al.* [1991].

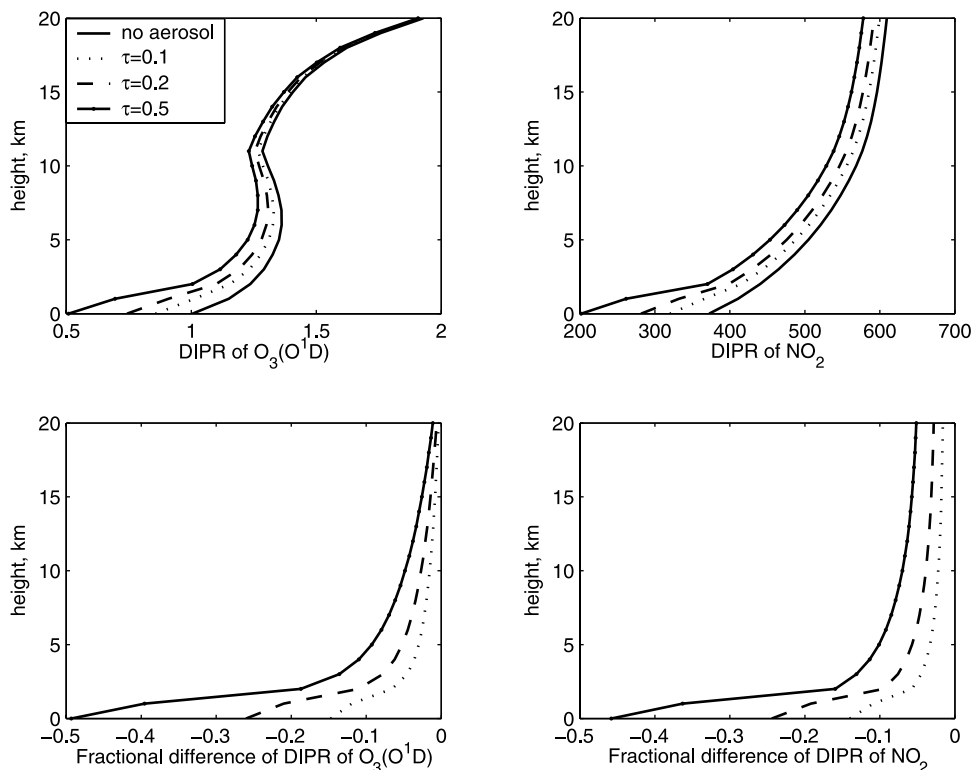
^bA 30% sea-salt solution.

with height and becomes very small at high levels. This is because the absorption by O_3 in the atmosphere affects the DIPR of $O_3(O^1D)$ more strongly than the DIPR of NO_2 , whose active wavelength upper limit is far beyond that of the O_3 UV absorption spectrum. (We can also see from Figure 9 that when the BC aerosol layer is located higher in the atmosphere, the impact on the whole photochemistry system is stronger.) This is because the layers in and below the aerosol layer are most affected.

[17] Figure 2 shows that at a NO_x concentration of 100 ppt, ozone production/destruction and OH concentration are decreased by $\sim 45\%$ at 990 mbar for an optical depth of 0.5, comparable to the change in DIPRs. The reductions of the chemical terms at optical depths 0.2 and 0.1 are about 24% and 13%, respectively. The fractional change of the chemical terms is smaller at lower NO_x than at higher NO_x concentration. It is also smaller than the fractional change of the DIPRs at higher altitudes (not shown), partly because of the lower temperature and humidity at the upper level. Another point from Figure 2 is that although the fractional changes of the chemical

terms do not change rapidly with the change of the concentration of NO_x , the absolute magnitudes are strong functions of NO_x since O_3 is destroyed when NO_x concentration is low, and produced when NO_x concentration is high. Moreover, high NO_x and high BC concentrations are correlated since BC is emitted from combustion sources, and combustion is also a big source of NO_x emission. However, the BC impact on the net tendency is less than the individual production or destruction terms because of partial cancellation.

[18] The sensitivity study will become more meaningful when we look at the BC concentrations in the atmosphere. The BC aerosol concentration is 0.2–2.0 $\mu\text{g}/\text{m}^3$ in the background continental areas, and 5–20 ng/m^3 in the remote oceans [Seinfeld and Pandis, 1998]. It is 1.5–20 $\mu\text{g}/\text{m}^3$ in urban areas with an average around 3.8 $\mu\text{g}/\text{m}^3$, and average PM10 (particles with diameter less or equal to 10 μm) BC values exceeding 10 $\mu\text{g}/\text{m}^3$ are common for some urban locations [Seinfeld and Pandis, 1998]. From Table 3 and the above sensitivity experiments, it can be seen that the BC impact is weak in remote

**Figure 1.** Sensitivity of the DIPR of $O_3(O^1D)$ and NO_2 to BC aerosol.

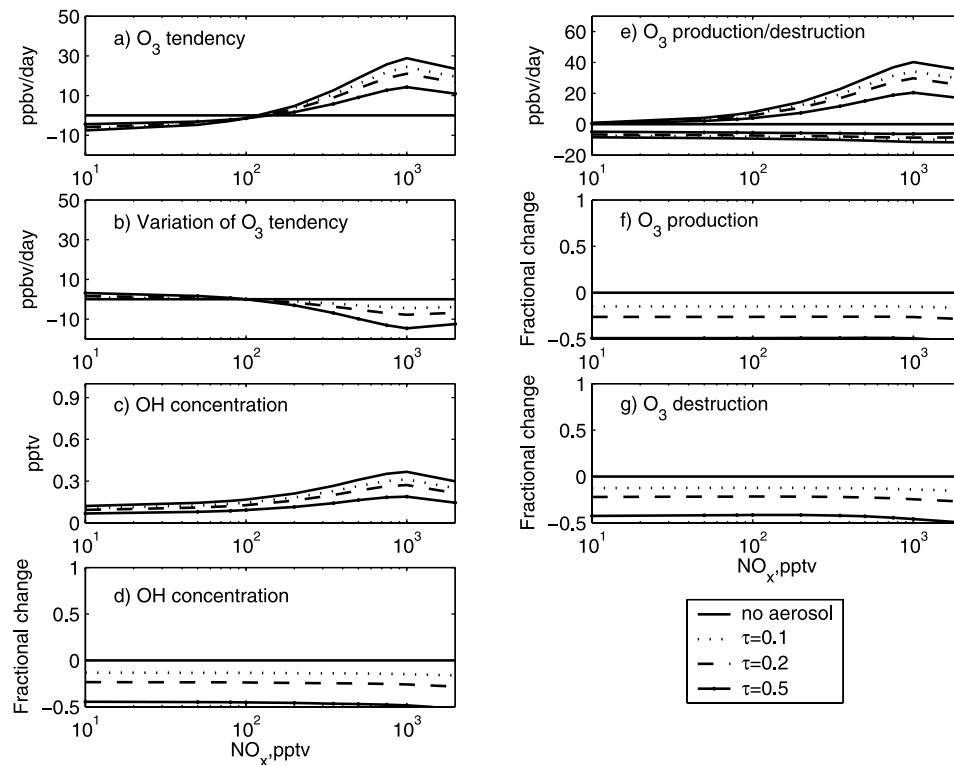


Figure 2. (a–g) Sensitivity of O_3 tendency and OH concentration to BC aerosol.

areas, where the BC optical depth is usually far below 0.05. The average BC impact in urban areas is around -10% , which corresponds to a BC concentration of $3.8 \mu\text{g}/\text{m}^3$, and is nearly -40% at the surface level in heavily polluted urban areas having the upper limit BC concentration of $20 \mu\text{g}/\text{m}^3$. Moreover, if we use a smaller BC particle density (for example, $1.0 \text{ g}/\text{cm}^3$, as used by Haywood *et al.* [1997] and Cooke *et al.* [1999]), the impact will be larger, since the number concentration, and therefore the optical depth, will be larger with the same BC mass concentration. This conclusion is consistent with that of He and Carmichael [1999], who found that the presence of absorbing aerosols in the boundary layer, which is mainly soot, could inhibit near-ground ozone formation and reduce ground level ozone by up to 70% in polluted environments.

3.3. Sensitivity to Mineral Dust Aerosol

[19] Mineral dust aerosol is a weaker absorber than BC aerosol. Figure 3 shows that at an optical depth of 0.5, dust aerosol decreases the DIPR of $O_3(O^1D)$ and NO_2 by nearly 35% at the surface level. The DIPRs are decreased about 17% and 10% at optical depth 0.2 and 0.1, respectively. The impacts decrease rapidly with height in the aerosol layer, and continue to decrease but more slowly above the aerosol layer. The chemical terms decrease about the same fractions as the DIPRs.

[20] The mineral dust aerosol concentration over the desert ranges from $30 \mu\text{g}/\text{m}^3$ up to $9500 \mu\text{g}/\text{m}^3$ [d'Almeida *et al.*, 1991], depending on the prevailing atmospheric conditions. The desert dust size distribution is a trimodal lognormal distribution, while the long-range transport of dust is in the accumulation mode, which is studied in this

paper. Our calculations show that the difference in impacts caused by different size distribution is small for scattering aerosols, like sulfate, and large for absorbing aerosols, like BC. The optical characteristic of mineral dust is in between. Thus we could use the above results of the sensitivity study to get a qualitative idea of the impact of dust over the desert in terms of mass concentration. From Table 3 and the above analysis, it can be seen that the lower limit of $30 \mu\text{g}/\text{m}^3$ produces an optical depth of no more than 0.02, whose impact is thus less than 2%. At the upper limit of $9500 \mu\text{g}/\text{m}^3$, the optical depth is above 5.0, and thus blocks the whole photochemistry. Li *et al.* [1996] showed that the aerosol optical depth seldom dropped below 0.2 (at 550 nm) in April 1994 at Barbados, where dust in accumulation mode is the dominant aerosol constituent during the spring, summer and early autumn when dust events are most common. The highest recorded aerosol optical depth was 0.72 during a large dust event. So the negative impact at the surface level by long-range transport dust is around 17% in dust seasons, and could reach nearly 50% in severe dust events. However, the absolute impact on O_3 will depend on NO_x , which does not correlate with dust like BC that does. The background dust concentrations in average continental and marine environments are at the lower limit of desert and long-range transport, whose optical depth is no more than 0.02. Moreover, the general lack of a strong correlation of dust with NO_x further weakens its impact on tropospheric chemistry.

3.4. Sensitivity to Sulfate and Oceanic Aerosols

[21] Sulfate and oceanic aerosols are very weak absorbers, acting instead as scatterers. Figure 4 shows that at an optical depth of 0.5, the negative effect of sulfate aerosol

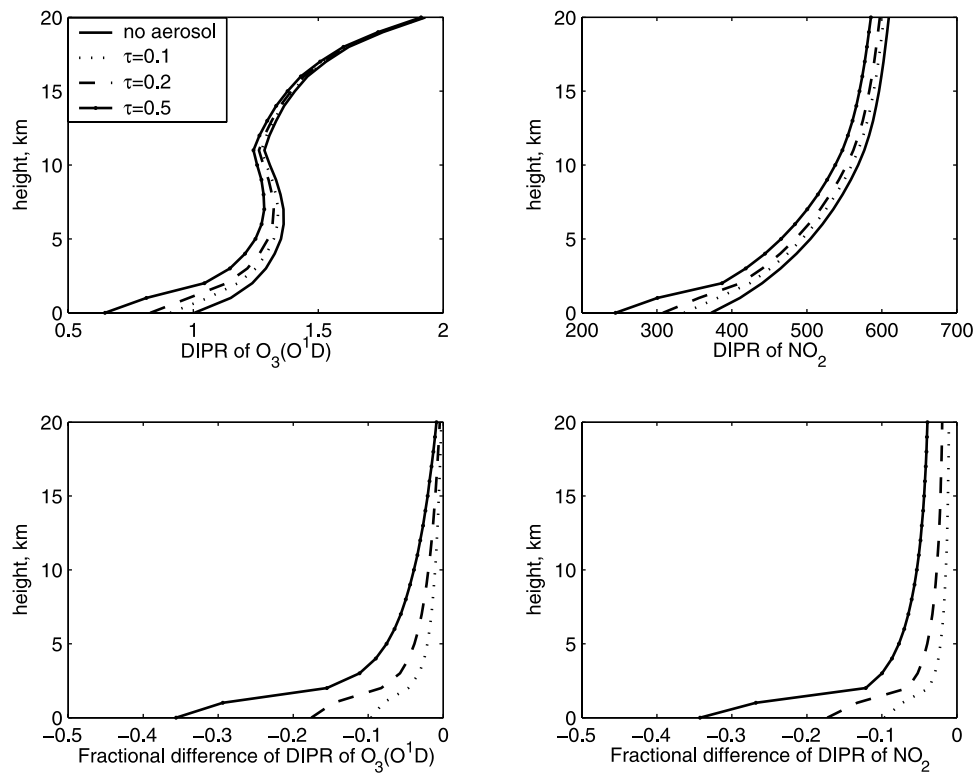


Figure 3. Sensitivity of the DIPR of $O_3(O^1D)$ and NO_2 to mineral aerosol.

on DIPRs is less than 5% at the surface level. The impact becomes positive within the first aerosol layer. The largest positive impact is achieved at the top of aerosol layer, which is around 8%. The negative impact at the surface level is

around 1% at the optical depth of 0.1, and is around 2% at the optical depth of 0.2. Figure 5 shows that oceanic aerosol behaves very similarly to sulfate aerosol, in the sense that both of them decrease the DIPRs by small fraction at the

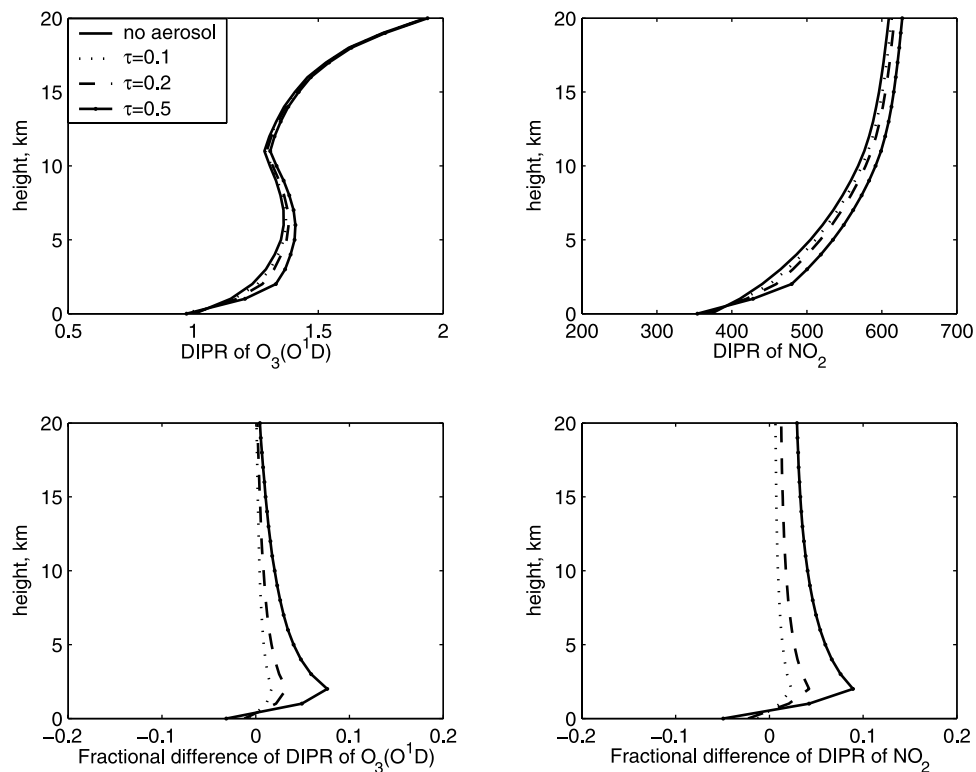


Figure 4. Sensitivity of the DIPR of $O_3(O^1D)$ and NO_2 to sulfate aerosol.

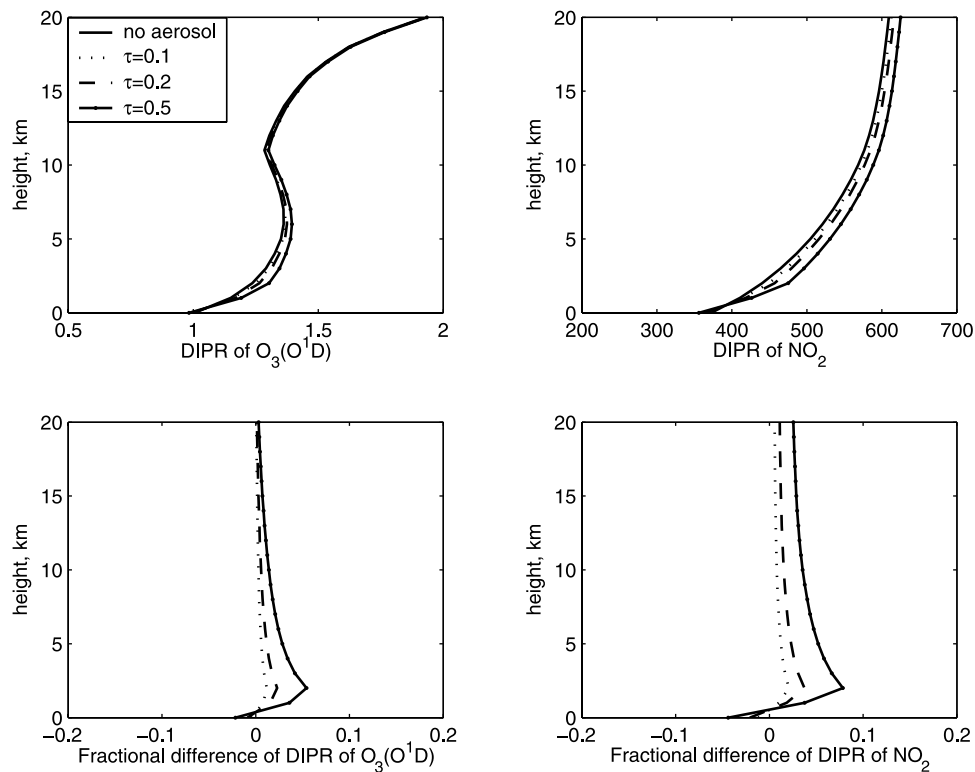


Figure 5. Sensitivity of the DIPR of $O_3(O^1D)$ and NO_2 to sea-salt aerosol.

surface level, and increase the DIPRs within the first aerosol layer.

[22] The anthropogenic sulfate loading can be as high as 50 mg/m^2 [Seinfeld and Pandis, 1998] in some urban areas, which is equivalent to an optical depth of ~ 0.25 . The background concentration is much smaller than this. The representative sea-salt aerosol concentration is around $20 \text{ }\mu\text{g/m}^3$ [Li et al., 1996; Jaenicke, 1993], which gives an optical depth of 0.02 from Table 3. Comparing the above numbers with those in Table 3, one would say that the impact of sulfate aerosol in some urban areas is around -2% at the surface level, and 4% at the top of sulfate aerosol layer. The impact is much smaller in remote areas. The impact of oceanic aerosols is generally less than 1% . Furthermore, from the fact that nitrate concentrations are comparable to sulfate [e.g., Adams et al., 1999], and organic carbon is comparable to BC [Cooke et al., 1999], one would say that all the scattering aerosols have modest or weak direct impacts on tropospheric photochemistry.

3.5. Sensitivity to Clouds

[23] Cloud aerosols are strong scatterers. Figure 6 shows that both DIPRs decrease 48% at the surface level under a cloud layer with an optical depth of 16.0. The DIPRs decrease 30% and 17% for optical depths of 8.0 and 4.0, respectively. The decreases do not change much from the ground level to the bottom of cloud layer. Within the cloud layer, the DIPR variations quickly change from negative to positive. The largest DIPR variation is achieved at the top of cloud layer: The DIPRs are increased about 50% , 35% , and 20% for optical depths of 16.0, 8.0, and 4.0, respectively. The fractional change is not linear, because linearity is only

valid at small optical depths. The positive fractional variations decrease above the cloud layer, but are still fairly large even at an optical depth of 4.0, especially the DIPR of NO_2 . Figure 7 shows that at 990 mbar and NO_x of 100 ppt, clouds with an optical depth of 16.0 gives about a 46% decrease in O_3 production/destruction and OH. The fractional decrease of the chemical terms is around 28% and 15% at optical depths of 8.0 and 4.0, respectively.

[24] The global mean cloud optical depth is around 5.0 [Rossow and Schiffer, 1991], which can produce an average decrease of $\sim 20\%$ for both the DIPRs and chemical terms at the ground level. Cloud optical depths above 8.0 are very common in the storm track zones in the middle latitude areas and in the intertropical convection zone (ITCZ) in tropical areas, which means that cloud impacts $\sim 30\%$ happen frequently in these regions. However, the relation between high NO_x levels and high cloud optical depths depends strongly on the region with potentially strong positive correlations in midlatitude storm tracks in the Northern Hemisphere and strong negative correlations in the ITCZ over the oceans.

3.6. Synergy Impacts of Clouds and Absorbing Aerosols

[25] Figure 8 shows the impacts when there are separate BC aerosol and cloud layers, located from the surface level to 2 km, and 2 km to 4 km, respectively. It appears that there is very little synergy under this circumstance. The DIPR is decreased $\sim 30\%$ by the cloud layer with an optical depth of 8.0, and 25% by the BC layer with an optical depth of 0.2 at the surface level. When BC and cloud layers are both present, the DIPRs are decreased $\sim 50\%$ at the surface level.

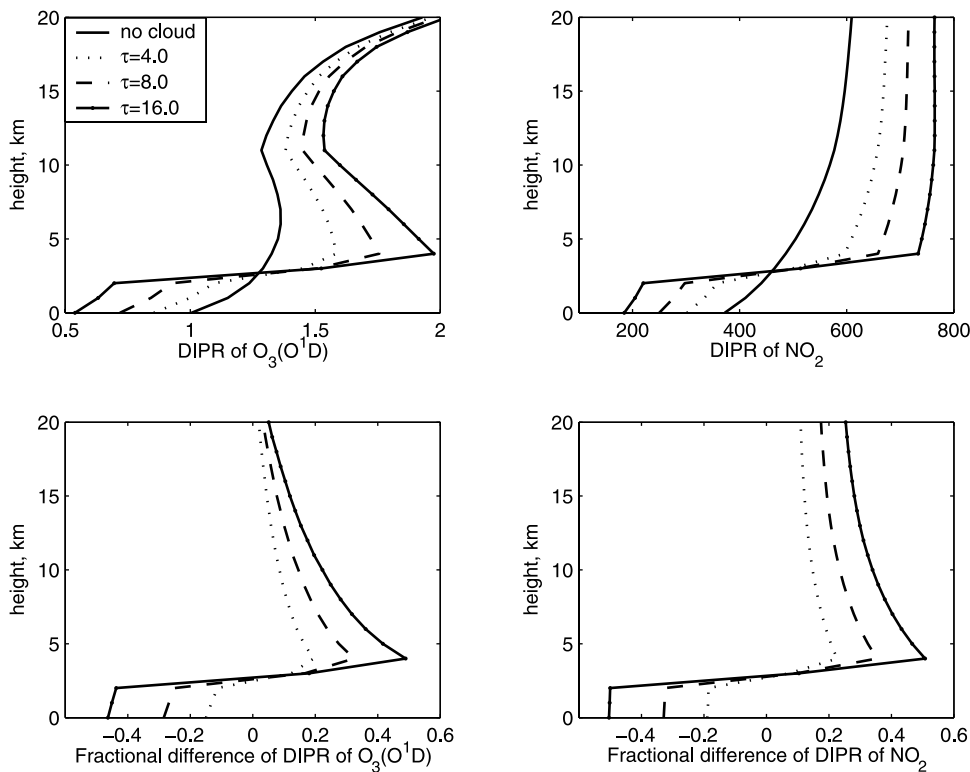


Figure 6. Sensitivity of the DIPR of $O_3(O^1D)$ and NO_2 to clouds.

The impact behaves similarly at higher levels. Another calculation shows that when the BC layer and cloud layer are collocated, for instance from the surface level to 2 km, the BC absorption effect is strengthened in and above the

aerosol layer, compared with the first case. There is a strong synergy when the cloud layer is located below the aerosol layer (Figure 9). The reduction due to the absorbing aerosol dominates in this case, and it cannot be captured by just

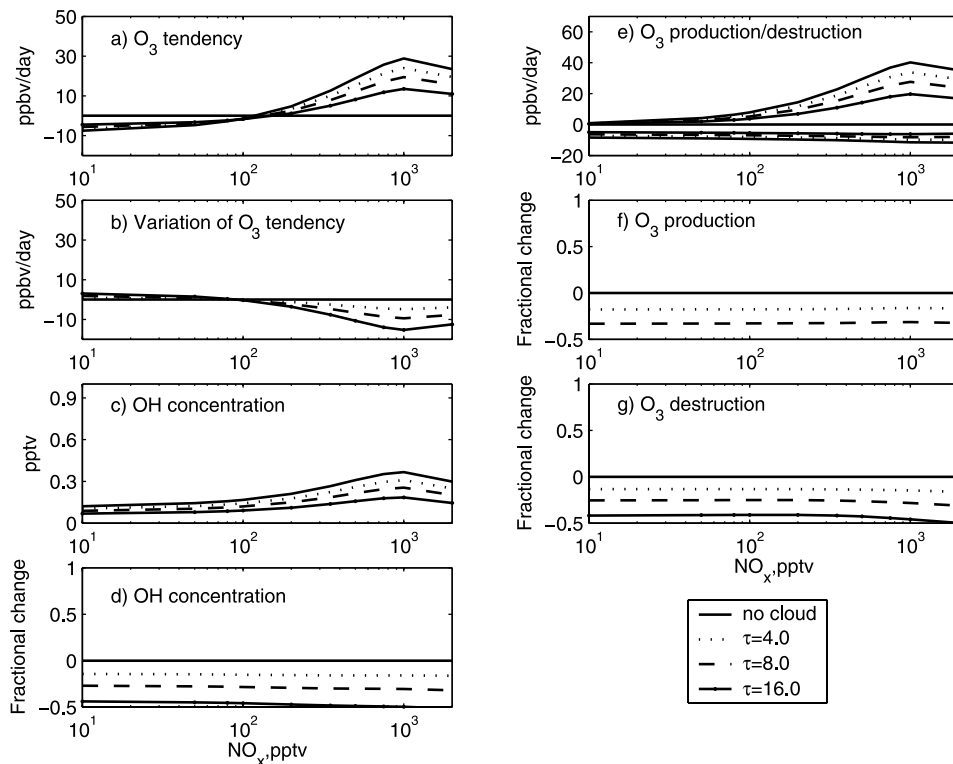


Figure 7. (a–g) Sensitivity of O_3 tendency and OH concentration to clouds.

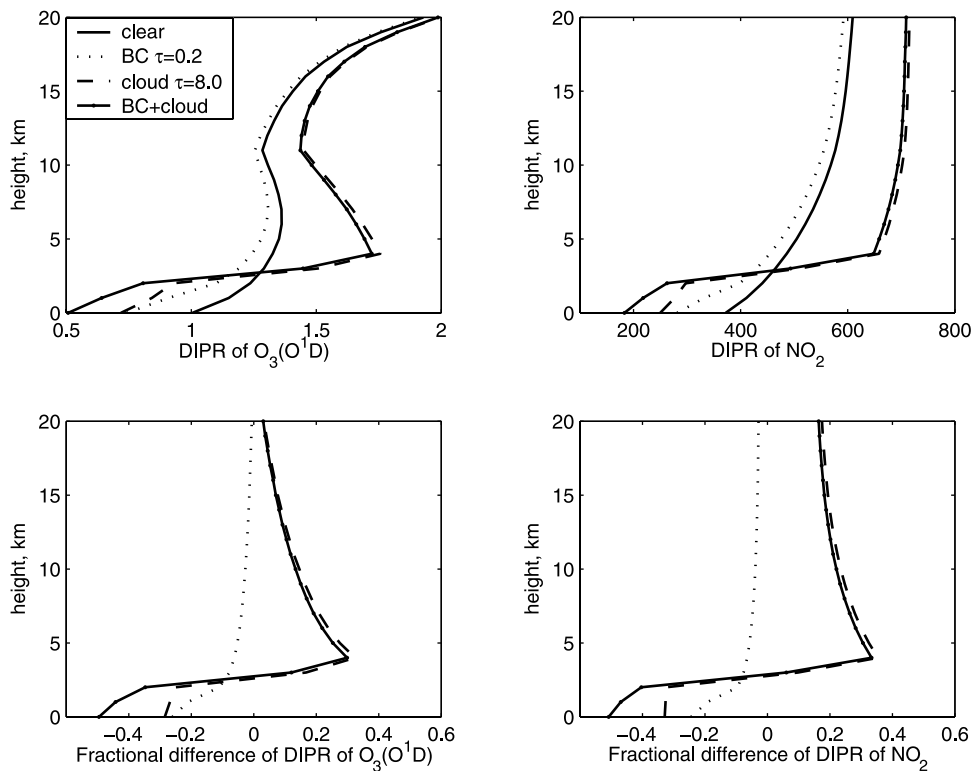


Figure 8. Impacts on the DIPR of $O_3(O^1D)$ and NO_2 when the BC layer is located under the cloud layer. BC layer, 0–2 km; cloud layer, 2–4 km.

adding the impacts of clouds and aerosol. This is consistent with the findings of *Haywood et al.* [1997] for direct radiative forcing.

4. Impacts of Different Aerosol Mixing States

[26] The aerosol mixing state is related to aerosol age [*Hitzenberger and Tohno*, 2001]. Freshly emitted aerosol particles are usually externally mixed, and aged particles are generally internally mixed. Coating is a special case of internal mixing, with one component acting as the core and the other as shell. As stated in the introduction section, the mixing state of BC determines its optical characteristics [*Ackerman and Toon*, 1981; *Bergstrom et al.*, 1982; *Chylek et al.*, 1984; *Jacobson*, 2001]. Therefore it is important to know the impacts produced by the different mixing states of BC with other scattering aerosols, like sulfate.

[27] External mixing averages the optical parameters of each aerosol component via a linear summation [*d’Almeida et al.*, 1991]:

$$\tau = \sum_{i=1}^n \tau_i, \quad \omega = \sum_{i=1}^n \omega_i \frac{\sigma_{ei}}{\sigma_e}, \quad g = \sum_{i=1}^n g_i \frac{\sigma_{si}}{\sigma_s}.$$

Here, τ_i , σ_{ei} , and σ_{si} are the optical depth, extinction cross section, and scattering cross section of each component, σ_e and σ_s are the summation of extinction cross section and scattering cross section of each component, respectively. For a pure scatter, $\sigma_e = \sigma_s$, because there is no absorption; otherwise, $\sigma_e = \sigma_s + \sigma_a$, where σ_a is the absorption cross section. For internal mixing we obtain the overall refractive

index by averaging the refractive index of each aerosol component according to its volume [e.g., *Chylek et al.*, 1981; *Haywood and Shine*, 1995]:

$$m_r = \sum_{i=1}^n m_{ri} \frac{V_i}{V}, \quad m_i = \sum_{i=1}^n m_{ii} \frac{V_i}{V}.$$

V_i is the volume of each aerosol component, and V is the total aerosol volume. m_{ri} and m_{ii} are the real and imaginary parts of the refractive index of each aerosol component. The coating case separates two different components into core and shell, and then uses a Mie calculation scheme to obtain the aerosol optical parameters.

[28] In the following calculation, the volume ratio of sulfate to BC is fixed at seven, which represents BC aerosol in urban areas that are not directly affected by local sources (e.g., in Uji and Vienna, measured by *Hitzenberger and Tohno* [2001]). The size distribution of sulfate is treated the same as BC in the external calculation. Thus both the number concentration and volume ratio of sulfate are seven times that of BC. Internal mixing and coating treat the aerosol as a mixture of BC and sulfate, with each particle composed of 12.5% BC and 87.5% sulfate by volume. In the coating scheme, BC is treated as the core.

[29] Figure 10 shows that an external mixture of BC and sulfate causes the smallest decrease in surface-level DIPRs. Internal mixing and coating produce almost the same reduction. Both are larger than external mixing, because with the same volumes of BC and sulfate, internal mixing and coating absorb more efficiently, and thus produce larger reductions. This is in agreement with the results of

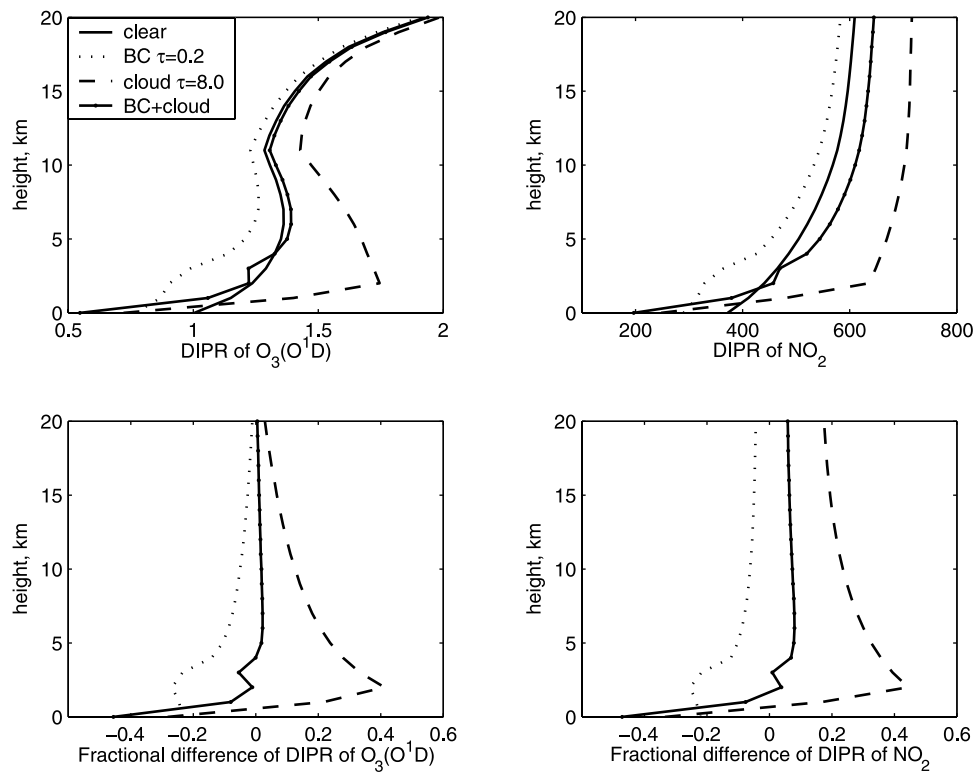


Figure 9. Impacts on the DIPR of $O_3(O^1D)$ and NO_2 when the BC layer is located above the cloud layer. BC layer, 2–4 km; cloud layer, 0–2 km.

Haywood et al. [1997]. Since our focus here is the relative impact produced by different mixing states, we set the BC number concentration at $1.0e^5/cm^3$ and the sulfate number concentration $7.0e^5/cm^3$ in the example shown in Figure 10,

values which are several times higher than the typical urban condition [*Whitby, 1978; Jaenicke, 1993*]. In Figure 10, the DIPR of $O_3(O^1D)$ is decreased 33.6% at the surface level, and the DIPR of NO_2 is decreased $\sim 30.7\%$ by external

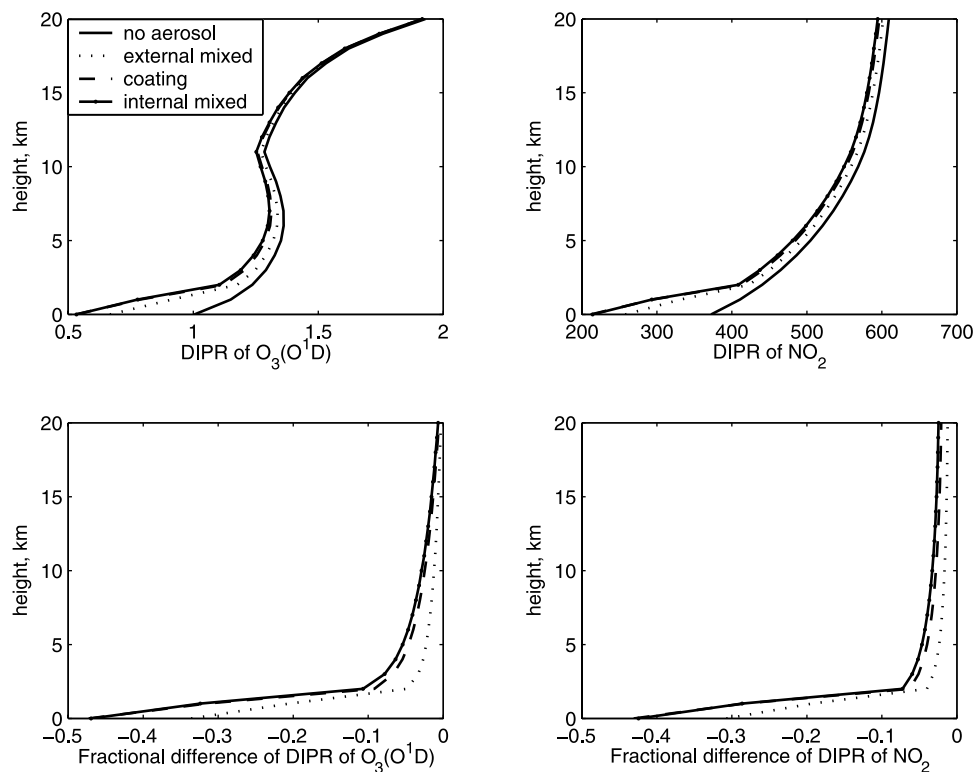


Figure 10. Impacts on the DIPR of $O_3(O^1D)$ and NO_2 when BC and sulfate are mixed differently.

mixing. The internal mixing state produces a 47.3% reduction of DIPR of O₃(O¹D), and 43.1% reduction of DIPR of NO₂. The difference between internal and external mixing decreases with height because there is more absorption at lower levels. The differences for O₃ tendency and OH concentration are the same as for the DIPRs at 990 mb. Additional calculations with sulfate to BC volume ratios of ~15, which represents remote areas [Haywood and Shine, 1995], show that the differences between internal and external mixing are even larger. The above results demonstrate that it is important to consider the mixing state of BC along with other scattering aerosol components.

5. Summary and Conclusion

[30] We have studied the sensitivities of photodissociation rate coefficients and O₃ photochemical tendencies to aerosols and clouds by employing a Mie code, a radiative transfer code (TUV) and a box chemistry code. This study shows that clouds and BC aerosol have the highest impact on tropospheric photochemistry. Both of them have strong regional effects on photochemistry because of their inhomogeneous distributions. Mineral dust aerosol has a modest impact on photochemistry, and the impact of sulfate aerosols is less. The impact of oceanic aerosol is the smallest among all the factors studied. The fractional change of the chemical terms is independent of NO_x. However, the absolute impacts depend on the concentration of NO_x. When NO_x is very low, the impacts on chemistry are very weak even if the DIPRs are strongly affected. Generally high levels of BC and NO_x are positively correlated, while the correlation between high NO_x and cloud optical depth varies by region. There is very little synergy between cloud and BC when clouds are located above the BC aerosol layer. The BC absorption effect will be strengthened when the cloud and BC layers overlap in altitude. There is a strong synergy when BC is located above the cloud layer, where the absorption by BC dominates. When BC is externally mixed with sulfate, its impact is ~70% of that produced by an internal mixing state at a sulfate and BC volume ratio of 7, and the difference increases when the volume ratio increases. BC coated with sulfate produces almost the same impact as internal mixing.

[31] This study finds that it is important to include the impact of BC aerosol on tropospheric photochemistry, especially in urban areas and biomass burning areas. The mixing state of BC with other scattering aerosol components should also be accounted for, since the BC impact on tropospheric photochemistry may be underestimated if only external mixing is applied. Another implication is that future tropospheric ozone concentrations will be even higher than today if BC concentrations are reduced while the concentrations of ozone precursors, NO_x and VOC, are kept at the same level. We note that it is the emission, not the concentration level, that people control. As pointed out by one of the anonymous reviewers, the lifetime of NO_x determines the level of NO_x for a given emission, and the change in lifetime depends on the relative change in JNO₂ and JO₃(O¹D). Our chemistry model, which uses a fixed NO_x, does not include this feedback.

[32] **Acknowledgments.** We wish to acknowledge the valuable comments of L. Horowitz, V. Ramaswamy, and B. Soden. The comments by the two anonymous reviewers were also very helpful. H. Yang wishes to thank the Atmospheric and Oceanic Sciences Program in Princeton University for its support. The grant number is NA17RJ2612.

References

- Ackerman, T. P., and O. B. Toon (1981), Absorption of visible radiation in atmosphere containing mixtures of absorbing and nonabsorbing particles, *Appl. Opt.*, **20**, 3661–3668.
- Adams, P. J., J. H. Seinfeld, and D. M. Koch (1999), Global concentrations of tropospheric sulfate, nitrate, and ammonium aerosol simulated in a general circulation model, *J. Geophys. Res.*, **104**, 13,791–13,823.
- Bergstrom, R. W., T. P. Ackerman, and L. W. Richards (1982), The optical properties of particulate elemental carbon, in *Particulate Carbon: Atmospheric Life Cycle*, edited by G. T. Wolff and R. L. Klimisch, pp. 43–51, Plenum, New York.
- Berner, A., S. Sidla, Z. Galambos, C. Kruijs, R. Hitzenberger, H. M. ten Brink, and G. P. A. Kos (1996), Modal character of atmospheric black carbon size distributions, *J. Geophys. Res.*, **101**, 19,559–19,565.
- Boucher, O., and T. L. Anderson (1995), General circulation model assessment of the sensitivity of direct climate forcing by anthropogenic sulfate aerosols to aerosol size and chemistry, *J. Geophys. Res.*, **100**, 26,117–26,134.
- Brasseur, G., and S. Solomon (1986), *Aeronomy of the Middle Atmosphere*, D. Reidel, Norwell, Mass.
- Chylek, P., V. Ramaswamy, R. J. Cheng, and R. G. Pinnick (1981), Optical properties and mass concentrations of carbonaceous smokes, *Appl. Opt.*, **20**, 2980–2985.
- Chylek, P., V. Ramaswamy, and R. J. Cheng (1984), Effect of graphitic carbon on the albedo of clouds, *J. Atmos. Sci.*, **41**, 3076–3084.
- Cooke, W. F., C. Liou, H. Cachier, and J. Feichter (1999), Construction of a 1° × 1° fossil fuel emission data set for carbonaceous aerosol and implementation and radiative impact in the ECHAM4 model, *J. Geophys. Res.*, **104**, 22,137–22,162.
- d'Almeida, G. A., P. Koepke, and E. P. Shettle (1991), *Atmospheric Aerosols, Global Climatology and Radiative Characteristics*, A. Deepak, Hampton, Va.
- Haywood, J. M., and K. P. Shine (1995), The effect of anthropogenic sulfate and soot aerosol on the clear sky planetary radiation budget, *Geophys. Res. Lett.*, **22**, 603–606.
- Haywood, J. M., D. L. Roberts, A. Slingo, J. M. Edwards, and K. P. Shine (1997), General circulation model calculations of the direct radiative forcing by anthropogenic sulfate and fossil-fuel soot aerosol, *J. Clim.*, **10**, 1562–1577.
- He, S., and G. R. Carmichael (1999), Sensitivity of photolysis rates and ozone production in the troposphere to aerosol properties, *J. Geophys. Res.*, **104**, 26,307–26,324.
- Hitzenberger, R., and H. Puxbaum (1993), Comparison of the measured and calculated specific absorption coefficients for urban aerosol samples in Vienna, *Aerosol Sci. Technol.*, **18**, 323–345.
- Hitzenberger, R., and S. Tohno (2001), Comparison of black carbon (BC) aerosols in two urban areas: Concentrations and size distributions, *Atmos. Environ.*, **35**, 2153–2167.
- Jacobson, M. Z. (2001), Strong radiative heating due to the mixing state of black carbon in atmospheric aerosols, *Nature*, **409**, 695–697.
- Jaenicke, R. (1993), Tropospheric aerosols, in *Aerosol-Cloud-Climate Interactions*, edited by P. V. Hobbs, Academic, San Diego, Calif.
- Klonecki, A. (1999), Model study of the tropospheric chemistry of ozone, Ph.D. thesis, Princeton Univ., Princeton, N. J.
- Klonecki, A., and H. Levy II (1997), Tropospheric chemical ozone tendencies in CO-CH₄-NO_y-H₂O system: Their sensitivity to variations in environmental parameters and their application to global chemistry transport model study, *J. Geophys. Res.*, **102**, 21,221–21,237.
- Krol, M. C., and M. V. Weele (1997), Implications of variations in photodissociation rates for global tropospheric chemistry, *Atmos. Environ.*, **31**, 1257–1273.
- Li, X., H. Maring, D. Savoie, K. Voss, and J. M. Prospero (1996), Dominance of mineral dust in aerosol light-scattering in the North Atlantic trade winds, *Nature*, **380**, 416–419.
- Liao, H., Y. L. Yung, and J. H. Seinfeld (1999), Effects of aerosols on tropospheric photolysis rates in clear and cloudy atmospheres, *J. Geophys. Res.*, **104**, 23,697–23,707.
- Madronich, S. (1987), Photodissociation in the atmosphere: 1. Actinic flux and the effects of ground reflections and clouds, *J. Geophys. Res.*, **92**, 9740–9752.
- Madronich, S., and S. Flocke (1998), The role of solar radiation in atmospheric chemistry, in *Handbook of Environmental Chemistry*, edited by P. Boule, pp. 1–26, Springer-Verlag, New York.

- Martin, R. V., D. J. Jacob, R. M. Yantosca, M. Chin, and P. Ginoux (2003), Global and regional decreases in tropospheric oxidants from photochemical effects of aerosols, *J. Geophys. Res.*, *108*(D3), 4097, doi:10.1029/2002JD002622.
- Matthijssen, J., K. Suhre, R. Rosset, F. L. Eisele, R. L. Mauldin III, and D. J. Tanner (1998), Photodissociation and UV radiative transfer in a cloudy atmosphere: Modeling and measurements, *J. Geophys. Res.*, *103*, 16,665–16,676.
- Nemesure, S., R. Wagener, and S. E. Schwartz (1995), Direct shortwave forcing of climate by the anthropogenic sulfate aerosol: Sensitivity to particle size, composition, and relative humidity, *J. Geophys. Res.*, *100*, 26,105–26,116.
- Peixoto, J. P., and A. H. Oort (1991), *Physics of Climate*, Am. Inst. of Phys., New York.
- Rossow, W. B., and R. A. Schiffer (1991), ISCCP cloud data products, *Bull. Am. Meteorol. Soc.*, *72*, 2–20.
- Seinfeld, J. H., and S. N. Pandis (1998), *Atmospheric Chemistry and Physics: From Air Pollution to Climate Change*, pp. 700–708, John Wiley, Hoboken, N. J.
- Whitby, K. (1978), The physical characteristics of sulfur aerosols, *Atmos. Environ.*, *12*, 135–159.
- World Climate Programme (1986), A preliminary cloudless standard atmosphere for radiation computation, *WCP-112, WMO/TD 24*, World Meteorol. Organ., Geneva.
-
- H. Levy II, Geophysical Fluid Dynamics Laboratory, P. O. Box 308, Princeton, NJ 08542, USA.
- H. Yang, Atmospheric and Oceanic Sciences Program, Princeton University, Princeton, NJ 08542, USA. (hyy@princeton.edu)